ABSTRACT BOOK

EMALLIA CONFERENCE

RIKEN-HOKKAIDO UNIVERSITY-PUSAN NATIONAL UNIVERSITY-NIMS

Busan, 7th – 8th of September 2017

INVITED TALK #1

Excitations of Higgs ferromagnetic phase in $Yb_2Ti_2O_7$

Lieh-Jeng CHANG[1]

[1]*Department of Physics, National Cheng Kung University, Tainan 70101, Taiwan*

$Yb_2Ti_2O_7$ with pyrochlore structure shows ferromagnetic phase transition at T_c = ~0.2 K. Above T_c, the compound is realized to be a quantum spin ice state which exhibits two-in-two-out classical spin ice spin configuration together with the quantum fluctuation of the magnetic components perpendicular to the <111> Ising axis. Below T_c, Yb^{3+} possesses moment of ~1.3 μB and points to [100] orientation. However, this ferromagnetic ground state is sample-dependent and can only be observed in high quality single crystals or polycrystalline samples [1]. This fact leads the difficulty of the study of $Yb_2Ti_2O_7$ in the past one and a half decades, and causes the constructions of theoretical frames incompletely.

I will be on behalf of our collaborative group to present our studies on our $Yb_2Ti_2O_7$ crystal showing ferromagnetic ground state below ~0.2 K. Besides our earlier studies by using polarized neutron scattering, μSR [2], low temperature magnetization [3] and heat capacity, synchrotron x-rays, we have also carried out inelastic neutron scattering experiments to further investigate low energy excitations in the same $Yb_2Ti_2O_7$ crystal. Below T_c, a broad mode at ~0.2 meV with little dispersion is observed along the <111> direction on LET, ISIS. This mode corresponds to the localized quantum spin ice monopole excitations. While at the pinch point (111), the collective monopole excitations with energy gap ~0.04 meV is seen in the backscattering spectra from DNA, J-PARC. On the other hand, at ~0.35 K, i.e. above T_c, only gapless continuum excitations are revealed in the experiments [4]. Preliminary results of neutron scattering in fields will be addressed. TEM had also been adapted to clarify the sample-dependent issue [5].

References:
[1] L. J. Chang, *et al.*, Nat. Commun. **3**, 992 (2012).
[2] L. J. Chang *et al*., Phys. Rev. B **89**, 184416 (2014).
[3] E. Lhotel *et al*., Phys. Rev. B **89**, 224419 (2014).
[4] L. J. Chang *et al*., to be published (2017).
[5] A. Mostaed *et al.*, Phys. Rev. B **95**, 094431 (2017).

E-mail for corresponding author: ljchang@mail.ncku.edu.tw

TALK #1

Strong interactions between graphene and platinum

Jinwoong Hwang[1], Hwihyeon Hwang[1], Min-Jeong Kim[1], Hyejin Ryu[2], Ji-Eun Lee[1], Qin Zhou[3], Sung-Kwan Mo[3], Jaekwang Lee[1], Alessandra Lanzara[4,5] and Choongyu Hwang[1,†]

[1] *Department of Physics, Pusan National University, Busan 46241, South Korea*

[2] *Advanced Light Source, Lawrence Berkeley National Laboratory, Berkeley, CA 94709, USA*

[3] *Mechanical and Materials Engineering, University of Nebraska, Lincoln, Nebraska 68588, USA*

[4] *Materials Sciences Division, Lawrence Berkley National Laboratory and Department of Physics, University of California, Berkeley CA 94720, USA*

[5] *Department of Physics, University of California, Berkeley CA 94720, USA*

Strong electronic correlations have been a fascinating theme in condensed matter physics over the past decades. Moreover, the graphene is considered as a powerful candidate to search for the strong electronic correlations due to the two-dimensional nature and Dirac fermionic behavior of charge carriers. Indeed, when the graphene is placed on *h*-BN, Wiedemann-Franz law is broken by strong electron-electron interaction in graphene [*Science*, **351**, 6277 (2016)]. In addition, it is possible to effectively control the electron-electron interaction in graphene via dielectric substrates [*Sci. Rep.*, **2**, 590 (2012)]. For that reason, we have investigated the electron band structure of a graphene/platinum interface using angle-resolved photoemission spectroscopy. The presence of platinum strongly influences the electronic properties of graphene, e.g., deep hole-doping of graphene and strong hybridization between graphene π and platinum 5*d* bands. Furthermore, the electron band structure of graphene near Fermi energy deviates from the one obtained within the local density approximation, despite graphene is standing on a metallic substrate. The graphene/platinum interface provides a unique platform to utilize the intrinsic properties of both graphene and platinum, in striking contrast to all the other graphene on metallic substrates.

† corresponding e-mail: chhwang@pusan.ac.kr

TALK #2

Possible coexistence of *s*- and *d*-wave pairing symmetry in λ-$(BETS)_2GaCl_4$ studied by μSR

Dita Puspita Sari[1,2], R. Asih[1,2], K. Hiraki[3], Y. Ishii[4], T. Takahashi[3], T. Koretsune[5], H. Seo[6], T. Nakano[2], I. Watanabe[1,7], and Y. Nozue[2]

[1]Advanced Meson Science Laboratory, RIKEN Nishina Center, Japan
[2]Department of Physics, Osaka University, Japan
[3]Department of Physics, Gakushuin University, Japan
[4]Department of Physics, Shibaura Institute of Technology, Japan
[5]Department of Physics, Tohoku University, Japan
[6]Condesed Matter Theory Laboratory, RIKEN, Japan
[7]Department of Condensed Matter Physics, Hokkaido University, Japan

The Cooper pairing mechanism of the organic superconductor λ-$(BETS)_2GaCl_4$ has attracted interest owing to the strongly correlated nature of this system lying near the Mott insulating phase [1]. A recent specific heat measurement reported a *d*-wave pairing symmetry, whereas the material has a different Fermi surface shape from the typical organic superconducting system κ-$(ET)_2X$ [2].

We present our recent experimental results of muon spin relaxation and rotation conducted at RIKEN-RAL Muon facility in the UK. By applying transverse fields (TF) 30 G and 60 G the flux line lattice is formed in the randomly aligned sample and then a bunch muon sensitively feels how magnetic penetration depth $\lambda(T)$, which is directly related to the superfluid density $\rho(T)$, is changing down to 0.3 K. The result in the TF = 30 G (the pink solid point shown in Fig. 1.) is hardly fitted by a simple *s*- or *d*-wave gap structure (fitting is not shown here).

Furthermore, it is clear in the TF of 60 G that another component might coexist since the low temperature data points still show a slight decrease of penetration depth at about 900 nm as shown in Fig. 1. We expect that the pairing symmetry is a coexistence of *s*-(dominant) and *d*-wave.

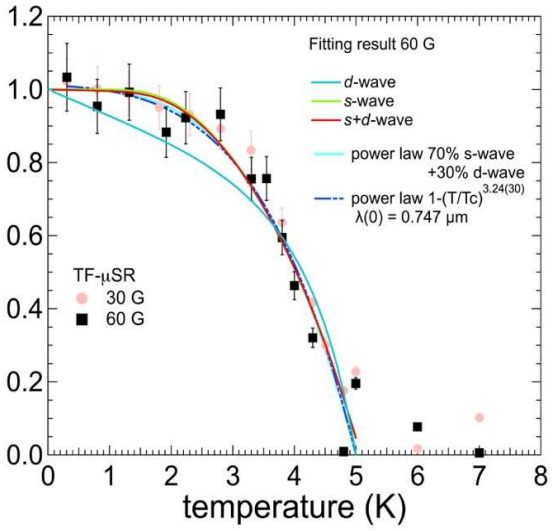

Figure 1. The black solid points are TF data at 60 G, plotted as normalized superfluid density $[\rho(T)/\rho(0)]^2 = [\lambda(0)/\lambda(T)]^2$ along with some tests of pairing symmetry fitting.

References

[1] H. Kobayashi *et al*., *Phys*. *Rev*. *B* **56**, 8526(R) (1997).
[2] S. Imajo *et al., J. Phys. Soc. Jpn.* **85**, 043705 (2016).

TALK #3

Newman-Janis Algorithm on Asymptotically Flat Spacetimes

Tadashi Sasaki
Division of Physics, Graduate School of Science,
Hokkaido University, Sapporo 060-0810, Japan

The Newman-Janis algorithm was originally discovered as a curious transformation which generate a rotating black hole solution of the Einstein equation from a non-rotating one[1]. The algorithm has been generalized to several classes of solutions[2][3], where the transformation typically takes the following form:

$$u' = u + iT(\theta,\phi), \quad r' = r + \frac{i}{2}D^2T(\theta,\phi), \quad \theta' = \theta, \quad \phi' = \phi,$$

where i is the imaginary unit, T is a function on S^2, and D is covariant derivative on S^2. Although there are several examples for the algorithm, the physical reason why such a complex transformation can work is not known.

Interestingly, the above form of transformation resembles that of the BMS supertranslation[4],

$$u' = u + \alpha(\theta,\phi) + O(r^{-1}), \quad r' = r + \frac{1}{2}D^2\alpha(\theta,\phi) + O(r^{-1}), \quad \theta' = \theta, \quad \phi' = \phi,$$

where $\alpha(\theta,\phi)$ is an arbitrary function on S^2. The supertranslation is one of the BMS transformations, which is the symmetry of asymptotically flat spacetimes and has recently been studied as a key ingredient for solving the black hole information loss problem.

Is this similarity accidental or not? For the first step to answer this question, we have investigated whether the Newman-Janis-like complex transformation can apply to asymptotically flat spacetimes or not. We applied generalized complex transformation

$$u' = u + U(\theta,\phi), \quad r' = r + R(\theta,\phi), \quad \theta' = \theta, \quad \phi' = \phi,$$

to asymptotically flat spacetime, and obtaind a condition for the resultant spacetime to be a solution of the Einstein equation,

$$i\partial_z\left[\mathrm{Im}R - \frac{1}{2}D^2\mathrm{Im}U\right] + \partial_u\sigma_{(0)}\partial_{\bar{z}}\mathrm{Re}U = 0,$$

where $z = e^{i\phi}\cot(\theta/2)$ is the stereographic coordinate on S^2 and $\sigma_{(0)}$ is called asymptotic shear.

If we consider the same transformation as the original NJ algorithm, that is, $\mathrm{Re}U = \mathrm{Re}R = 0$, then the condition reduces to $\mathrm{Im}R = D^2\mathrm{Im}U/2 + \text{const.}$, which is almost the same relation as the previously known examples for NJ algorithm up to a constant.

Finally, we will discuss the possibility for unified understanding of the BMS symmetry and the Newman-Janis algorithm, and future perspectives.

References

[1] E. T. Newman and A. I. Janis, J. Math. Phys. **6** 915 (1965)
[2] C. J. Talbot, Commun. math. Phys. 13, 45-61 (1969)
[3] H. Erbin, arXiv:1701.00037[gr-qc]
[4] H. Bondi, F.R.S., M. G. J. van der Burg, and A. W. K. Metzner, Proc. Roy. Soc. Ser. A, **269**, 21-52 (1962)
[5] S. W. Hawking, M. J. Perry, and A. Strominger, Phys. Rev. Lett. **116**, 231301 (2016)

TALK #4

Self-restraint of spin-fluctuation-mediated superconductivity in iron-based superconductors

Tomoaki Agatsuma and Hiroyuki Yamase

Graduate School of Science, Hokkaido University, and
National Institute for Materials Science

Superconductivity occurs close to the electronic nematic phase in a typical phase diagram of iron-based superconductors [1]. Nematic fluctuations are thus expected to play an important role to understand iron-based superconductors. In fact, the nematic fluctuations turn out to drive superconductivity with transition temperature comparable to experiments [2, 3]. In particular, intra-Fermi-pocket scatterings of electrons due to large nematic fluctuations are vital to the superconductivity and the other scattering processes such as inter-Fermi-pocket scatterings also work cooperatively.

On the other hand, the spin-density-wave phase also realizes close to the superconducting phase in iron-based superconductors [1]. Hence it is natural that spin fluctuations are also important for superconductivity. In this mechanism, superconductivity is driven by spin fluctuations with momenta around $(\pi, 0)$ and $(0, \pi)$, which connect different Fermi pockets [4]. While the important role of such spin fluctuations is well established, we have found that seemingly tiny intra-Fermi-pocket scatterings reduce considerably the onset temperature of superconductivity. Moreover, the instantaneous magnetic interaction, which is often neglected, is also crucially important for the onset of superconductivity. Our findings suggest that spin fluctuations restrain themselves from achieving high-T_c superconductivity, in contrast to the case of the nematic fluctuations.

References :
[1] G. R. Stewart, Rev. Mod. Phys. 83, 1589 (2011).
[2] H. Yamase and R. Zeyher, Phys. Rev. B 88, 180502(R) (2013).
[3] T. Agatsuma and H. Yamase, Phys. Rev. B 94, 214515 (2016).
[4] I. I. Mazin, D. J. Singh, M. D. Johannes and M. H. Du, Phys. Rev. Lett. 101, 057003 (2008).

TALK #5

Magnetic ordered states of hole doped pyrochlore iridates $(Nd_{1-x}Ca_x)_2Ir_2O_7$ studied by μSR

R. Asih,[1,2] J. Angel,[1,3] S. Maeda,[4] D. P. Sari,[1,2] F. Astuti,[1,3] K. Matsuhira,[4] M. Wakeshima,[3] Y. Hinatsu,[3] I. Watanabe,[1,2,3] T. Nakano,[2] and Y. Nozue[2]

RIKEN Nishina Center[1], Dept. of Phys. Osaka Univ.[2], Dept. of Phys. Hokkaido Univ.[3], Kyushu Institute of Technology[4]

Pyrochlore iridates, $R_2Ir_2O_7$ (R = Y or lanthanide elements), have recently attracted growing interest because of their potential for realizing new topological states, such as Dirac semimetal, Axion insulator, and Weyl semimetal. These systems provide an ideal platform to an interplay the relation between the electron-electron correlation (U) and the spin-orbit coupling (SOC) in which U can be systematically tuned by changing the ionic radius of R^{3+} ion [1]. In particular, abundant emergent quantum states have been theoretically predicted on the boundary of the metal insulator transition (MIT) which lies between R = Nd and Pr [1]. Therefore, it is required to finely control U by the chemical substitution on $Nd_2Ir_2O_7$. Pure $Nd_2Ir_2O_7$ exhibits the metallic behavior at high temperature and undergoes MIT at temperature of T_{MI} = 33 K [2]. μSR study on $Nd_2Ir_2O_7$ indicated a long-range magnetic order of Ir^{4+} moments below T_{MI}, followed by an additional magnetic order of Nd^{3+} moments below 10 K [3, 4].

We report μSR study on magnetic ordered states of $(Nd_{1-x}Ca_x)_2Ir_2O_7$ to investigate changes in magnetic ordered states of Ir^{4+} and Nd^{3+} moments by the Ca^{2+} substitution for Nd^{3+} which leads to the doping of holes in the Ir 5*d* band. As the Ca concentration increases, MIT is rapidly suppressed. As shown in Fig. 1 (a), the hole doping suppressed the onset of magnetic order and the internal field originating from Ir^{4+} moments. A critical slowing down in the relaxation rate [Fig. 1 (b)] was observed at about 10 K indicating an additional magnetic order of Nd^{3+} moments appeared. A possible of quantum criticality is found to engender in this hole-doped system. The detail results of the μSR results on $(Nd_{1-x}Ca_x)_2Ir_2O_7$ will be presented in the talk.

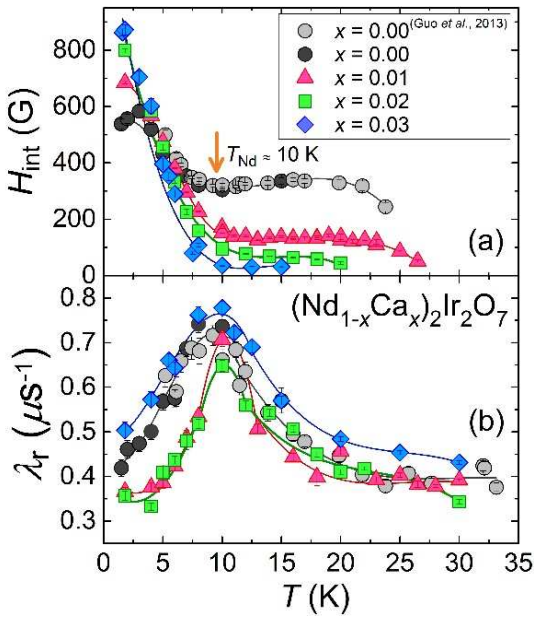

Fig. 1. Temperature dependences of the (a) internal field at muon sites and (b) relaxation rate in $(Nd_{1-x}Ca_x)_2Ir_2O_7$

Reference

[1] X. Wan *et al.*, Phys. Rev. B **83**, 205101 (2011)
[2] K. Matsuhira *et al.,* J. Phys. Soc. Jpn. **80,** 094701 (2011)
[3] H. Guo *et al.,* Phys. Rev. B **88**, 060411(R) (2013)
[4] R. Asih *et al.,* J. Phys. Soc. Jpn. **86,** 024705 (2017)

INVITED TALK #2

Magnetotransport studies of carbon-based nanotubes by use of non-contact method

Yugo Oshima

RIKEN, Condensed Molecular Materials Laboratory

It is well-known that the electronic structure of single-walled carbon nanotubes (SWCNT) is determined by the band structure of the graphene sheet and the periodic boundary conditions of the wave functions along the tube's circumference. For this reason, it is thought that structural differences in the SWCNTs or the magnetic field effect yield remarkable differences in the transport and magnetotransport properties. However, due to the non-negligible contact resistance, it is extremely difficult to observe the intrinsic transport properties of SWCNTs. Furthermore, contact between SWCNTs yield extrinsic effects such as the variable range hopping transport or weak localization effect.

To get rid of such extrinsic effects and observe the genuine magnetotransport properties of SWCNTs, we have employed the cavity perturbation technique, which is a non-contact method to evaluate the conductivity, to a highly-oriented thin film of SWCNTs with low concentration. And we have succeeded to observe the Aharonov-Bohm effect of both metallic and semiconducting SWCNTs [1].

In my talk, I will briefly explain about this non-contact method for evaluating the magnetotransport, and present the results of highly-aligned thin films of SWCNTs. Moreover, we have varied the concentration of the SWCNTs in the thin film to study systematically the effect of contact between the tubes. These results will also be presented and its magnetotransport properties will be discussed.

[1] Y. Oshima *et al*., Phys.Rev. Lett. 104, 016803 (2010).

TALK #6

Chimera states in nonlocally coupled phase oscillators with higher harmonic interaction

Division of Physics, Hokkaido Univ.

Yusuke Suda, Koji Okuda

Under the balance of inflow and dissipation of energy, there often appear nonlinear oscillators in various natural or artificial systems. In many cases, these oscillators interact with one another, and compose a many-body system. Such systems are called coupled oscillator systems, and studied numerously in a wide range of scientific fields for many years [1].

Synchronization is a famous phenomenon as a typical collective behavior of oscillators, while there often appears a strange phenomenon called the chimera state, which is characterized by the coexistence of the coherent synchronous and the incoherent not-synchronous regions, in nonlocally coupled phase oscillators [2]

$$\frac{\partial}{\partial t}\theta(x,t) = \omega - \int_{-\pi}^{\pi} dx'\, G(x-x')\, \Gamma(\theta(x,t) - \theta(x',t)), \tag{1}$$

where $\theta(x)$ is 2π-periodic phase on one-dimensional space $x \in [-\pi, \pi]$ under the periodic boundary condition and ω is the natural frequency. The coupling kernel function $G(x)$ characterizes nonlocal coupling. The interaction between oscillators is described as the coupling function Γ, and the sine coupling $\Gamma(\phi) = -\sin(\phi + \alpha)$ with phase lag parameter α is generally used. It is known that chimera states for Eq. (1) with the sine coupling, for example, as shown in Fig. 1(a) are spatial steady states which have steady mean fields. This steady mean field is a solution of the self-consistent equation [2].

In contrast, when we especially use the Hansel-Mato-Meunier coupling $\Gamma(\phi) = -\sin(\phi + \alpha) + r\sin(2\phi)$ where r is the amplitude ratio of the second harmonic component, chimera states become more complicated [3]. In this study, we study the properties of such chimera states numerically. For example, the mean field of the chimera state as shown in Fig. 1(b) is temporally periodic, namely, not steady, so the phase distribution in the incoherent regions change periodically. Furthermore, the coherent regions with different average frequencies exist together. These properties can not be seen for steady chimera states mentioned above.

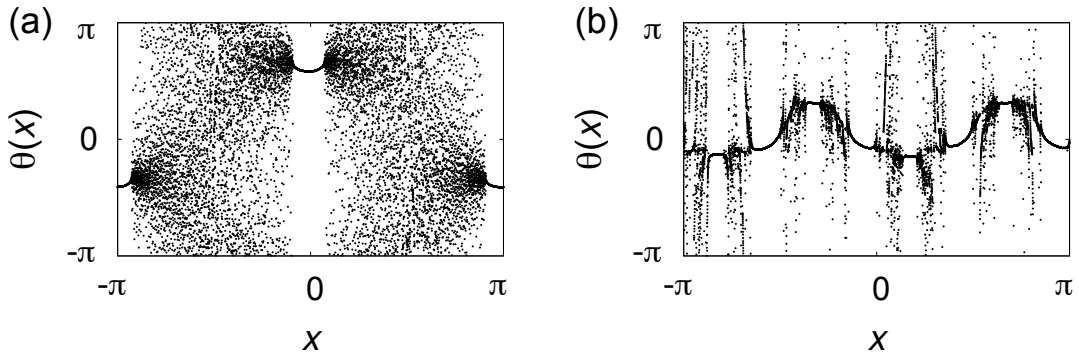

Figure 1: Chimera state in nonlocally coupled phase oscillators, Eq. (1). These figures show the snapshot of phase $\theta(x)$. As the coupling function Γ, (a) the sine coupling and (b) the Hansel-Mato-Meunier coupling are respectively used.

[1] Y. Kuramoto, *Chemical Oscillation, Waves, and Turbulence* (Springer, Berlin, 1984).
[2] Y. Kuramoto and D. Battogtokh, Nonlinear Phenom. Complex Syst. **5**, 380 (2002).
[3] Y. Suda and K. Okuda, Phys. Rev. E **92**, 060901(R) (2015).

TALK #7

Growth of electronically distinct manganite thin films by modulating cation stoichiometry

Sangkyun Ryu[1], Joonhyuk Lee[1], Eunyoung Ahn[1], Jiwoong Kim[1], Andreas Herklotz[2], Jong-Seong Bae[3], Ho Nyung Lee[2], Younghak Kim[4], Jae-Young Kim[4], Tae-Yeol Jeon[4], Jinhyung Cho[5], Sungkyun Park[1], and Hyoungjeen Jeen[1*]

[1]Department of Physics, Pusan National University, Busan 46241, Korea

[2]Materials Science and Technology Division, Oak Ridge National Laboratory, Oak Ridge, Tennessee 37831, USA

[3]Busan center, Korea Basic Science Institute, Busan 46742, Korea

[4]Pohang accelerator laboratory, Pohang University of Science and Technology, Pohang 37673, Korea

[5]Department of Physics Education, Pusan National University, Busan 46241, Korea

**E-mail: hjeen@pusan.ac.kr*

Pulsed laser deposition (PLD) is well-known for a stoichiometry transfer method in thin film growth. However, in some cases, it can create either anion or cation off-stoichiometry from the target materials by growth condition. To take advantage of this fact, we used $Nd_{1-x}Sr_xMnO_3$ as a model system and varied its growth condition such as oxygen partial pressure (PO_2) to make modulation of cation stoichiometry. In this work, we stabilized two electronically different $Nd_{0.5}Sr_{0.5}MnO_3$ thin films on (001) $(LaAlO3)_{0.3}$-$(SrAl_{0.5}Ta_{0.5}O_3)_{0.7}$ (LSAT) by varying PO_2. The electrical and magnetic properties of NSMO films were confirmed by transport and superconducting quantum interference device (SQUID) measurements. From x-ray absorption spectroscopy, we observed that valence states of Mn in NSMO films deposited higher PO_2 are lower valence state, and it is the origin of the difference of physical property. In addition, we checked the difference of ratio of cations (Nd and Sr) by x-ray photoelectron spectroscopy. This work was supported by the Basic Science Research Program through the NRF funded by the Ministry of Education (NRF-2015R1D1A1A020 62175).

TALK #8

Magnetically Ordered States in Hole-Doped Pyrochlore Iridate $Y_{1-x-y}Cu_xCa_yIr_2O_7$

J. Angel[1, 2], R. Asih[1, 3], R. Shibahara[4], K. Matsuhira[4], T. Sakakibara[5], I. Watanabe[1, 2, 3]
[1]RIKEN Nishina Center, [2]Hokkaido University, [3]Osaka University,
[4]Kyushu Institute of Technology, 5ISSP University of Tokyo

Pyrochlore iridates, $R_2Ir_2O_7$ (R = Y and lanthanides), are expected to exhibit nontrivial states such as Mott insulating, Weyl semi-metallic, axion insulating, and topological crystalline insulating ones because of its frustrated magnetic interactions [1,2]. The signature of quantum critical point (QCP) is expected to occur by the carrier doping to the system [3]. Based on transport and magnetic measurements, the metal-insulator transition (MIT) can be tuned by changing the R ionic radius [4].

$_{Y2}Ir_2O_7$ is predicted to be a Weyl semimetal with the all-in all-out magnetic ground state [1] followed by MIT around 165 K [2]. It is essential to understand the magnetic properties of pyrochlore iridates as their electronic structures are strongly coupled with the magnetic ground states [5]. Also, Ir is expected to play an important role. $Y_2Ir_2O_7$ is an ideal system to investigate Ir moments, especially to study the presence of QCP because the Y atom does not have a local magnetic moment. Fig. 1 is the temperature dependence of $Y_{0.95-x}Ca_xCu_{0.05}Ir_2O_7$ for x=0, 0.05, and 0.1. This result indicates that the electronic property became from insulating to be metallic by the Ca-doping. Fig. 2 shows the temperature dependence of the muon-spin relaxation rate, λ, measured on the sample with x=0.05 and y=0. In this sample, MIT is suppressed compared to that observed in the non-doped sample, but a magnetic transition is still observed. We are going to report and discuss changes in the magnetic property and electrical resistivity result of these compounds as the effect of Cu and Ca substitution.

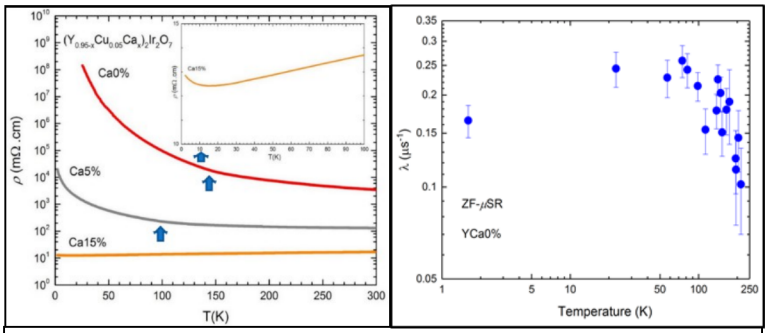

Fig.1 Electrical resistivity result of (Y0.95-xCaxCu0.05)2Ir2O7. Inset: magnification of YCa15%. The temperature of MIT for YCa0%, YCa5%, and YCa15% is about 150 K, 100 K, and 10 K, respectively.
Fig. 2 Zero-field time spectra of YCa0%

References:
[1] W. K. Zhu *et al.,* Phys. Rev. B **90**, 054419 (2014)
[2] H. Fukazawa and Y. Maeno, J. Phys. Soc. Jpn. **71**, 2578 (2002)
[3] L. Savary, E. Moon and L. Balents., Phys. Rev. X **4**, 041027 (2014)
[4] W. Witczak-Krempa *et al.*, Annual Review of Condensed Matter Physics, Vol. 5: 57-82 (2014)
[5] W. K. Zhu et al., Phys. Rev. B **90**, 054419 (2014)

TALK #9

Resistivity Measurement under pressure in pseudo-κ-(BEDT-TTF)$_4$[(H$_3$O)Ga(C$_2$O$_4$)$_3$]·C$_6$H$_5$NO$_2$

Dept. of Phys. Graduate School of Science Hokkaido Univ.
Kazuto MORIBE , Yosuke FUTAMI , Yoshihiko IHARA , Atsushi KAWAMOTO

Organic conductor (BEDT-TTF)$_4$[(H$_3$O)Ga(C$_2$O$_4$)$_3$]·C$_6$H$_5$NO$_2$ [BEDT-TTF(ET):bis(ethylenedithio)tetrathiafuluvalene] consists of conducting layers of ET molecules and insulating layers of anions alternately. There are two isomorphic materials β" type salt and pseudo-κ type salt. These salts have quasi-2-dimendional electronic system. These salts have the different packing structure of ET molecules. In the β" type salt, ET molecules are stacking parallel each other. In the pseudo-κ salt, one ET dimmer is surrounded by six monomers. The β"-type salt shows superconducting transition at 7 K [1]. On the other hand, the behavior of the temperature dependence of resistivity in pseudo-κ type salt is of insulator at ambient pressure. The band gap of pseudo-κ type salt can be estimated about 90 meV. The gap seems to be related to the charge ordering. We can estimate the charge distribution from the bonding length of central C=C bond [2]. The estimation of the charge on the ET molecules gives the value about +1 for rich ET molecules (dimers) and 0 for poor ET molecules (monomers). This distribution suggests the possibility of the difference of the physical properties. Therefore this salt is so interesting. In general, the transfer integral of ET molecules increases by applying pressures. This increase means that the band width becomes broad and the band gap can disappear. Therefore this salt has the possibility to become metal state by applying pressures. To investigate the behavior of the temperature dependence of resistivity under pressure and the relationship with superconducting state, we performed resistivity measurement under pressure using PPMS designed by Quantum Design. For this measurement, we developed a holder to mount a pressure cell on the PPMS. Fig. 1 shows the temperature dependence of resistivity at 1.3GPa and ambient pressure. The behavior of resistivity remains semiconducting behavior, but the absolute value of resistivity is suppressed by applying pressures. Now further measurement under pressures is in progress.

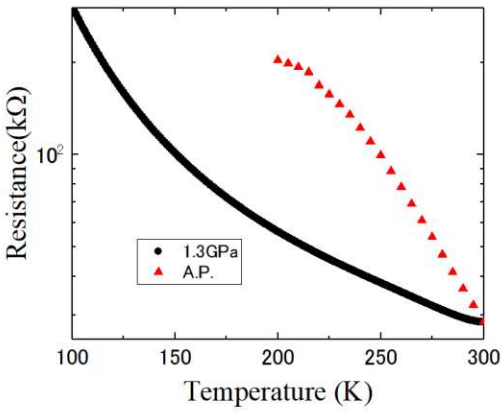

Fig. 1 Temperature dependence of R

[1] H.Akutsu *et al.* , J. AM. CHEM. SOC. (2002) **124**, 12430
[2] P.Guionneau *et al.* , Synthetic Metals (1997)**86**, 1973

TALK #10

Ab initio study of polaron dynamics in transition metal oxides

Taewon Min, Sehwan Song, Sungkyun Park* and Jaekwang Lee*

Department of Physics, Pusan National University, Busan 46241, South Korea

Abstract

In conventional semiconductors such as Si and Ge the band theory works very well. However in highly insulating materials like typical transition metal oxides, the band theory often fails because their band widths are extremely narrow, resulting in the slowing down of the electron motion. These slow moving electrons strongly couple with atoms in the solid materials, severely deforming the surrounding lattice and leading to localized states, and thus electrons are readily self-trapped by self-induced local lattice distortions. In this case, electronic transport is mostly dominated by polaron hopping from lattice site to lattice site rather than the drift motion. Here, we explore the polaron dynamics in transition metal oxides, particularly, Fe_2O_3 using density functional theory calculations and temperature dependent conductivity measurement. We find that the polaron hopping occurs only in the two dimensional FeO plane and its activation barrier is highly susceptible to the lattice deformation induced by intrinsic oxygen vacancy and extrinsic Sn dopant. Our combined studies show that the polaron dynamics in transition metal oxides can be controlled by selective substitution into Fe sites, which can provide important parameters for developing highly efficient Fe_2O_3-based electrochemical device.

TALK #11

Microscopic theory of the vortex-core charging in superconductors

Dept. of Phys., Hokkaido Univ.
M. Ohuchi, H. Ueki and T. Kita

The vortex-core charging in a type-II superconductor has been observed experimentally [1]. Although a number of studies on vortex-charging have been carried out by using the mean field theory of superconductivity such as the Bogoliubov–de Gennes (BdG) equations [2, 3], the BdG equations cannot clarify dominant contribution to the vortex-charging. In addition, it is difficult to incorporate Fermi-surface and gap anisotropies. On the other hand, all force terms for describing charging in superconductors is missing from the standard Eilenberger equations (i.e., the quasiclassical equations of superconductivity) that have been used to study superconductors in a magnetic field microscopically.

Recently, study on the flux-flow Hall effect has been carried out by using the augmented quasiclassical equations in the Keldysh formalism with the Lorentz and pair-potential gradient forces, which are effects of first order in quasiclassical parameter [4]. In addition, we have transformed the augmented quasiclassical equations into Matsubara formalism, so that charging in superconductors can be calculated microscopically and quantitatively [5]. However, the result obtained from the augmented quasiclassical equations may include an unreliable quantitative result depending on the parameter region, because the derivation of the equations have been performed by using the perturbation expansion in the quasiclassical parameter and the gradient expansion with the Moyal product.

We study the validity of the augmented quasiclassical equations by calculating the vortex-core charging of a two-dimensional s-wave superconductor in comparison with the result based on the BdG equations and clarify dominant contribution to the vortex-charging. Since the augmented quasiclassical equations has the possibility to clarify the transport phenomenon in type-II superconductors such as the flux-flow Hall effect in the presences of the spatial inhomogeneity and vortex motion, it is very important to verify the validity of the equation.

[1] K. Kumagai, K. Nozaki, and Y. Matsuda, Phys. Rev. B **63**, 144502 (2001).
[2] M. Matsumoto and R. Heeb, Phys. Rev. B **65**, 014504 (2001).
[3] M. Machida and T. Koyama, Phys. Rev. Lett. **90**, 077003 (2003).
[4] E. Arahata and Y. Kato, J. Low Temp. Phys. **175**, 346 (2014).
[5] M. Ohuchi, H. Ueki, T. Kita, J. Phys. Soc. Jpn. **86**, 073702 (2017).

INVITED TALK #3

Study of Spiro-Material as Hole Transport Layer to Enhance Performance of Dye Sensitized Solar Cell (DSSC)

Lusi Safriani, Winna P. Primawati, Afifah Nurrida, Sheila Sakkyananda, Tuti Susilawati, Cukup Mulyana and Annisa Aprilia

Departement of Physics, Padjadjaran University, Jl. Raya Bandung Sumedang Km. 21 Jatinangor, Sumedang 45363, Indonesia

Recently, Dye Sensitized Solar Cells (DSSC), a low-cost photovoltaic device, has received attention to be investigated although it is required further research to enhance its performance. DSSC was initiated in 1991 by O'Regan and Grätzel [1]. Some advantages of DSSC are their low-cost and simple manufacturing processes, lightweight, flexible and also low toxic [2]. One of factors that could inhibit the performance of DSSC is related to charge transport especially hole transport in porous TiO_2 layer. The incomplete pore-filling of hole transport materials into porous TiO_2, leads to poor dye-regeneration and reduces device efficiency [3]. A good candidate material for a transparent hole transport material is small molecules so it will be easy to penetrate into porous TiO_2 layer. Organic material based on spiro material has been used as hole transport material in DSSC due to its charge transport properties [4]. We used different kind of spiro-material i.e 2,2′,7,7′-tetra- kis(diphenylamino)-9,9′-spirobifluorene (spiro-TAD) and 2,2′,7,7′-tetra(m-tolylphenylamino) -9,9′-spirobi- fluorene (spiro-TPD) and 2,2′,7,7′-tetrakis(N,N-di-p-methoxyphenyl-amine)9,9′-spirobifluorene (spiro-OMeTAD) as hole transport layer to produce DSSC. We then performed current-voltage (J-V) characteristics measurement and calculated some of DSSC parameters i.e. ideally factor (n), series resistance (R_S), and shunt resistance (R_{SH}) which derived from current-voltage (J-V) curve using the simplify equation of ideal diode model. The influences of different kind of spiro-material to the solar cell performance will be completely discussed.

References

[1] O'Regan B and Gratzel M 1991 *Nature* 353 737
[2] Gratzel M 2006, *Prog. Photovolt: Res. Appl.* 14 429
[3] Wen Yuan, Hui Zhao, Gregory L. Baker 2014 *Organic Electronics* 15 3362–3369
[4] Tobat P. I. Saragi, Till Spehr, Achim Siebert, Thomas Fuhrmann-Lieker, and Josef Salbeck 2007 *Chem. Rev.* 107 1011−1065

TALK #12

Muon Sites in High-Tc Superconductor, $YBa_2Cu_3O_6$

Irwan Ramli[A,B], S.S. Mohd -Tajudin[A,C], Julia Angel[A,B], Harison B. Rozak[A,C], S. Sulaiman[C], M. I. Mohamed-Ibrahim[C] and I. Watanabe[A,B,C]

[A]RIKEN Nishina Center, [B]Hokkaido University, [C]Universiti Sains Malaysia

Since the discovery of high-Tc superconductivity, many experimental and theoretical studies have been done to understand the magnetic and electronic properties in order to describe the superconducting mechanism. We are approaching this matter from the study on the magnetic properties by using muon-spin-relaxation (μSR) technique [1,2]. Our aim is to understand hyperfine fields at the muon positions in materials by using the density functional theory (DFT) calculation methods. In order to discuss hyperfine interactions at the muon positions, the location of the stopped muon is necessary. Once we know about the muon positions, we can discuss the electronic structures surrounding muons and microscopic information of surrounding electronic magnetic moments [3]. We use the RIKEN's cluster-type supercomputing system named HOKUSAI GreatWave for our calculations [4].

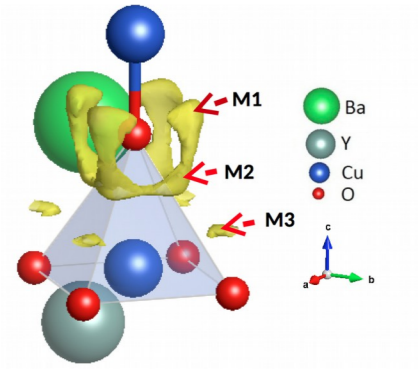

Figure1. Possible muon sites in YBa2Cu3O6 estimated from our DFT calculations.

We are investigating the muon sites in $YBa_2Cu_3O_6$ ($YBCO_6$). This system is a family of the Y-based high-Tc superconducting oxides which shows an antiferromagnetic state at room temperature. From our preliminary DFT calculations of the electrostatic potential, we found three possible muon positions as shown in Fig.1. We also took into account quantum effects such as local lattice distortions caused by the injected muon, the zero-point energy vibration and spatial spin distribution of the muon itself as a fine particle. In this presentation, we report in more detail, our progress in the determination of muon sites in $YBCO_6$ in conjunction with precise detailed dipole field calculations.

References:

[1] N. Nishida *et al.*: Jpn. J. appl. Phys. **26,** L1856 (1987).
[2] Y. Koike *et al.* : J. Phys. Soc. Jpn. **85**, 091006 (2016).
[3] P. Bonfá, *et al.*: J. Phys. Soc. Jpn. **85**, 091014 (2016).
[4] HOKUSAI GreatWave (2015): **http://www.riken.jp/pr/press/2015/20150403_1/**

TALK #13

Magnetic ordering in the Hubbard model with two types of antisymmetric spin-orbit couplings on a zigzag chain

Dept. of Phys., Hokkaido Univ.
M. Yatsushiro and S. Hayami

An effective antisymmetric spin-orbit coupling (ASOC), which originates from the atomic spin-orbit coupling without the inversion symmetry, has attracted since it gives rise to various fascinating phenomena, such as the Dirac electrons at the surface of topological insulator and noncentrosymmetric superconductivity. In these systems, spontaneous magnetic orderings lead to magnetoelectric phenomena, where the magnetization (electric polarization) is induced by an electric (magnetic) field, since time reversal symmetry is no longer presereved. Meanwhile, similar situations occur even in the centrosymmetric systems, e.g. a zigzag chain and honeycomb structure, where the inversion center is missing at each lattice site [1, 2]. Reflecting the lack of the inversion center at lattice sites, the ASOC is induced in a staggered way. Once the staggered magnetic ordering breaking the spatial inversion symmetry occurs, the uniform ASOC is activated, which results in similar magnetoelectric phenomena. Furthermore, the staggered magnetic ordering on such lattice structures simultaneously activates odd-parity multipoles, such as magnetic quadrupole and toroidal dipole [3]. Thus, it is intriguing problem to clarify when and how the magnetic orderings with odd-parity multipoles are stabilized in the fundamental model.

In this study, we focus on how the ASOC affects the magnetic orderings from the viewpoint of stability. We consider the minimal Hubbard model including the staggered ASOC on a one-dimensional zigzag chain [4]. By performing the mean field calculations, we obtain the ground-state phase diagram by changing the amplitude of the ASOC. In addition to the staggered ASOC, we consider the contribution of the uniform ASOC, which appears by the surface and domain effect. We show the parameter space where the magnetic orderings with odd-parity multipoles are realized and discuss how the band structures are modified under odd-parity multipoles.

[1] Y. Yanase: J. Phys. Soc. Jpn. **83** (2014) 014703.
[2] S. Hayami, H. Kusunose, and Y. Motome: Phys. Rev. B **90** (2014) 024432.
[3] S. Hayami, H. Kusunose, and Y. Motome: J. Phys.: Condens. Matter **28** (2016) 395601.
[4] Y. Yanase and H. Harima: Kotai Butsuri **46** (2011) 229-239; **46** (2011) 283-292; **47** (2012) 101-111.

TALK #14

The New Muon Spin Relaxation Functions for One-Two sources of Distributed Field on Muon Sites

Muhamad Darwis Umar [1,2)] **and Isao Watanabe**[1,2]

[1)]*RIKEN Nishina Center, 2-1 Hirosawa, Wako, Saitama 351-0198, Japan,*
[2)]*Department of Physics, Hokkaido University, Sapporo, Hokkaido, 060-0810, Japan,*

Lineshapes of muon spin relaxation functions for some materials, for instance a quasi one-dimensional spin-1/2 molecular chain [1] and spin gap antiferromagnetic materials: Spin-Peierls [2]-spin ladder [3,4], show neither purely Gaussian nor purely Gaussian. The distributed internal field on muon sites of these lineshape for both static or dynamics behaviour can be produced by one source or more. To get appropiate physical information of these materials via Muon Spin Spectroscopy, we use Kubo Golden Formula (KGR) to developed analytical muon spin relaxation functions for intermediate static field distribution for both one source and two-source cases. Our derivation for zero field cases corfirms the previous results [3] and proposes new analytical forms for zero field and applied longitudinal field cases. In our derivation, we can consistently show that KGR can be applied to longitudinal field cases included to recovery the known function for longitudinal field-Lorentzian Kubo-Toyabe (LF-GKT)[5].

$$P_\mu(B_{ext},t) = 1 + \frac{2\lambda^{2\beta}}{\omega_0^2(-\beta+3)(-2\beta+2)}\cos\omega_0 t\frac{\exp\left[-\frac{(\lambda t)^\beta}{\beta}\right]}{t^{-2\beta+2}} - \frac{2\lambda^\beta}{\omega_0}\left(1-\frac{1}{(-\beta+3)}\right)J_1(\omega_0 t)\frac{\exp\left[-\frac{(\lambda t)^\beta}{\beta}\right]}{\tau^{-\beta+1}}$$
$$- \frac{2\lambda^{2\beta}}{\omega_0^2(-\beta+3)(-2\beta+3)}J_0(\omega_0 t)\frac{\exp\left[-\frac{(\lambda t)^\beta}{\beta}\right]}{t^{-2\beta+2}} - \frac{2\lambda^{2\beta}}{(-2\beta+3)(-\beta+3)(-2\beta+2)\omega_0^2}\frac{\cos\omega_0 t\exp\left[-\frac{(\lambda t)^\beta}{\beta}\right]}{t^{-2\beta+2}}$$
$$- \frac{2\lambda^{3\beta}}{(-\beta+3)(-2\beta+3)\omega_0^2}\int_0^t J_0(\omega_0\tau)\frac{\exp\left[-\frac{(\lambda\tau)^\beta}{\beta}\right]}{\tau^{-3\beta+3}}d\tau - \frac{2\lambda^\beta}{(-\beta+3)}\int_0^t J_0(\omega_0\tau)\frac{\exp\left[-\frac{(\lambda\tau)^\beta}{\beta}\right]}{\tau^{-\beta+1}}d\tau$$
$$- \left(\frac{2\lambda^{2\beta}}{(-\beta+3)(-2\beta+2)}\right)\left(\frac{1}{(-2\beta+3)}-1\right)\int_0^t J_0(\omega_0\tau)\frac{\exp\left[-\frac{(\lambda\tau)^\beta}{\beta}\right]}{\tau^{-2\beta+1}}d\tau$$
$$- \frac{2\lambda^{3\beta}}{(-\beta+3)(-2\beta+2)\omega_0^2}\left(\frac{1}{(-2\beta+3)}-1\right)\int_0^t\cos\omega_0\tau\frac{\exp\left[-\frac{(\lambda\tau)^\beta}{\beta}\right]}{\tau^{-3\beta+3}}d\tau$$

$1 < \beta < 2$

$$P_\mu(B_{ext},t) = 1 - \frac{2\lambda^{3/2}}{3\omega_0}J_1(\omega_0 t)\tau^{1/2}\exp\left[-\frac{(\lambda\tau)^{3/2}}{3/2}\right] + \frac{4}{3}\frac{\lambda^3}{\omega_0^2}\int_0^t J_0(\omega_0\tau)\exp\left[-\frac{(\lambda\tau)^{3/2}}{3/2}\right]d\tau$$
$$- \frac{4}{3}\lambda^{3/2}\int_0^t J_0(\omega_0\tau)\tau^{1/2}\exp\left[-\frac{(\lambda\tau)^{3/2}}{3/2}\right] - \frac{4}{3}\frac{\lambda^3}{\omega_0^2}\int_0^t\cos(\omega_0\tau)\exp\left[-\frac{(\lambda\tau)^{3/2}}{3/2}\right]d\tau$$

$\beta = 1.5$

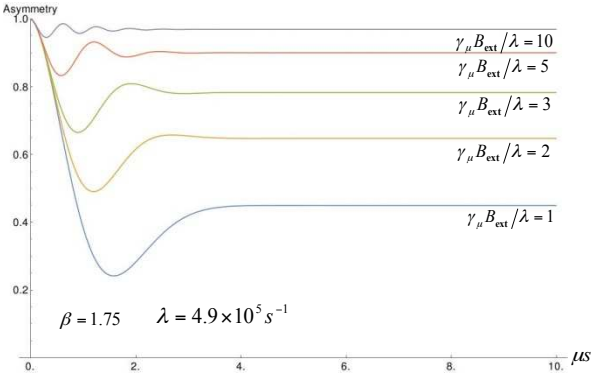

The muon spin relaxation function of one source-between Gaussian-Lorentzian distributions in longitudinal field plotted for the different ratio of applied field to width.

References

[1] T. Lancaster, *et. al.*, Phys. Rev. B 73, 020410(R) (2006)
[2] S. J. Blundel, *et al.*, J. Phys.: Condens. Matter 9, L119-L124 (1997)
[3] R. C. Williams, *et. al.*, Phys. Rev. B 93, 140406(R) (2016)
[4] M. I. Larkin, *et al.*, Phys. Rev. Lett. 85, 9, 1982 (2000)
[5] M.I. Larkin, *et al.*, Physica B, 289-290, 153-156 (2000)

TALK #15

Effect of thermal treatment on N^+ ions implanted NbO_2 thin films

Gowoon Kim[1], Eunyoung Ahn[1], Yu-Seong Seo[2], Jin-Hyung Cho[3] and Hyoungjeen Jeen[1,*]

[1] Department of physics, Pusan National University, Busan 46241, Korea

[2] Department of physics Sungkyunkwan university, Suwon, Gyeonggi-do 16419, Korea

[3] Department of physics education, Pusan National University, Busan 46241, Korea

Niobium oxides (NbO_x) can have various compositions due to multiple valence states of Niobium ions, resulting in different the optical and electrical properties of each NbO_x. For example, Nb_2O_5 shows insulating behavior with E_g = 3.4 eV, NbO_2 shows semiconducting behavior with E_g = 0.4-1 eV and NbO shows metallic behavior and superconducting behavior at low temperature. So NbO_x can be used as components in electronics and electrochemical devices.

In this work, we present epitaxial growth of NbO_2 and annealing effect on N^+ ions implanted NbO_2. Epitaxial NbO_2 thin films are prepared by RF magnetron sputtering on (0001) Al_2O_3 substrate. Using high resolution x-ray diffractometer (HRXRD), we confirmed (110) NbO_2 is stabilized on (001) Al_2O_3. Then, we implanted nitrogen ions into the NbO_2 films in Korea multi-purpose accelerator complex (KOMAC) and annealed at different temperature, ranged from 200°C to 450°C, for 2h at vacuum. From atomic force microscopy (AFM), we confirmed our epitaxial as-grown thin films are atomically flat but nitrogen ion implantation made surfaces rough. But, annealing made the rough surfaces back to smooth. In addition, we also observed that formation of new phase and modulation of the lattice constants of the existing NbO_2 after implantation and thermal treatment. To observe the change in chemical and optical properties, we used spectroscopic ellipsometry and x-photoelectron spectroscopy, respectively. We got the clear difference in the each spectra. The result of this study will be useful to understand the effect of nitrogen ions implantation on the tuning physical and chemical properties of epitaxial oxides. This research was supported by the Basic Science Research Program through the NRF funded by the Ministry of Education (NRF-2015R1D1A1A02062175).

TALK #16

Anomalous antiferromagnetic resonance of λ-(BETS)$_2$FeCl$_4$ in antiferromagnetic insulating phase

Taehoon Lee[1,2], Yugo Oshima[1,2], Hengbo Cui[1] and Reizo Kato[1]

RIKEN[1], Hokkaido University[2]

λ-(BETS)$_2$FeCl$_4$, where BETS is bis(ethylenedithio)tetraselenafulvalene, is a well-known charge transfer salt which shows a superconducting state at high magnetic field. This system is composed from the conducting π-electrons of BETS molecules and the magnetic *d*-electrons of Fe spins, and it is considered that strong interaction between the π- and *d*-electrons exists. While paramagnetic and metallic behaviors are observed in the high temperature phase, the system turn into an antiferromagnetic insulating (AFI) state below 8.3 K. It was previously believed that the metal to insulator transition of the π-electrons is due to the antiferromagnetic long-range order of the *d*-electrons. However, recent heat capacity measurement observed a huge excess specific heat below 8.3 K, and its origin was explained from the contribution of paramagnetic *d*-electrons [4]. It suggests that the *d*-electron remains paramagnetic below 8.3 K and only the π-electrons becomes antiferromagnetic and localized. However, this explanation is not consistent with the existence of strong π-*d* interaction, and contradicts with previous electron spin resonance (ESR) studies [1-3].

To have a better understanding of the AFI phase, we have performed ESR measurements. When the magnetic field is applied parallel to the easy-axis, we have observed the easy-axis mode of AFMR below 5 T, however, the easy-axis mode of AFMR changes to hard-axis mode of AFMR above 5 T (as shown Fig. 1). It suggests that a change of the easy-axis occurs above 5 T. This unconventional magnetic properties of λ-(BETS)$_2$FeCl$_4$ should be strongly connected with the electronic state of the π-electrons. Our ESR results will be presented in detail, and the AFI phase of λ-(BETS)$_2$FeCl$_4$ will be discussed.

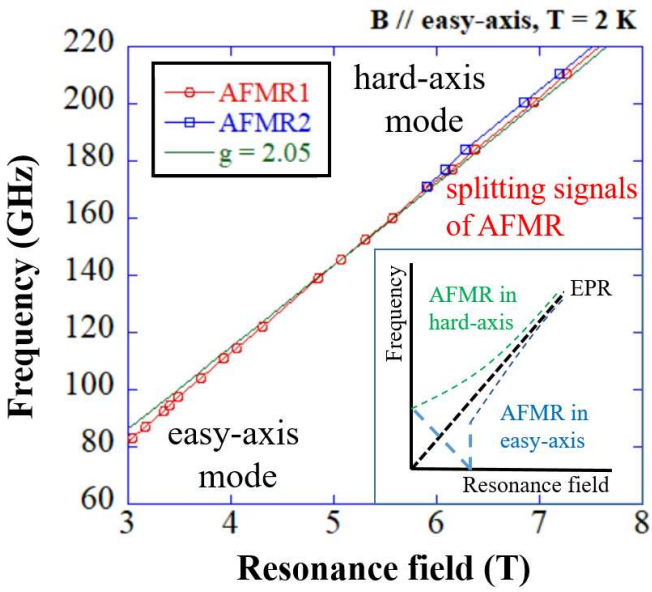

Fig. 1 : Frequency-field dependence of AFMR (B//*easy*-axis, T = 2 K) The inset shows frequency-field dependence of conventional AFMR

Reference
[1] I. Rutel *et al*., Phys. Rev. B **68** (2003) 144435
[2] L. Brossard *et al*., Eur. Phys. J. B **1** (1998) 439
[3] T. Suzuki *et al*., Phys. Rev. B **67** (2003) 020408(R)
[4] H. Akiba *et al*., J. Phys. Soc. Jpn. **78** (2009) 033601

TALK #17

Ground state of *M*-component Bose Einstein condensates with 3/2-body interactions

Wataru Kohno, Akimitsu Kirikoshi, Takafumi Kita

Department of Physics, Hokkaido University, Sapporo 060-0810, Japan,
e-mail: wataruv@phys.sci.hpkudai.ac.jp

As for describing weakly interacting BEC systems, Bogoliubov theory [1] has been widely accepted, which brings the approximated effective Hamiltonian by an order of *O(N)* (*N* : total-particle number) into diagonal form. This approximation provides us an interesting result that low-lying "quasi-particles" (single-particle modes) are equivalent with "phonons" (collective modes). In other words, this result indicates that the system behaves as a collection of non-interacting quasi-particles. Moreover, these modes satisfy with the strict theorem for the ground state of a BEC system given by Hugenholtz and Pines [2]. Thus, this theory has been used for BEC systems extensively as a physical approximation.

On the other hand, the contributions of *2*-body interactions (collisions between quasi-particles) and *3/2*-body interactions (collisions of two quasi-particles throws one of them into the condensate and visa versa) which should be incorporated self-consistently are neglected in Bogoliubov theory since the contributions are by an order of $O(N^{1/2})$. Girardeau and Arnowitt [3] constructed a variational wave function for the ground state of homogeneous systems to evaluate the ground-state energy incorporating *2*-body interactions of quasi-particles. However, this improvement caused an unphysical energy gap in the single-particle excitation spectrum unlike the Bogoliubov spectrum with a gapless linear dispersion and an infinite lifetime in the long-wavelength limit, which is in contradiction to the Hugenholtz–Pines theorem. With these backgrounds, a variational wave function for the ground state with the contributions of *3/2*-body interactions has been constructed recently [4]. This study shows that (i) the unphysical energy gap caused by *2*-body interactions is suppressed by considering *3/2*-body interactions and (ii) the width of the single-particle spectrum is finite even in the long-wavelength limit and thus the single-particle mode and the collective mode in a BEC system are distinguishable in terms of respective lifetimes.

In this presentation, we develop the variational method [4] and construct a ground-state wave function of weakly interacting *M*-component BECs. The method, results and considerations will be shown in detail in our presentation.

References

[1] N. N. Bogoliubov, *J. Phys*. (USSR) **11**, 23 (1947).
[2] N. M. Hugenholtz and D. Pines, *Phys. Rev.* **116**, 489 (1959).
[3] M. Girardeau and R. Arnowitt, *Phys. Rev.* **113**, 755 (1959).
[4] T. Kita, *J. Phys. Soc. Jpn.* **86**, 044003 (2017).

INVITED TALK #4

Valley-symmetric quasi-1D carrier guiding in ballistic graphene

Hu-Jong Lee

Department of Physics, POSTECH, Korea

hjlee@postech.ac.kr

Recent progress in preparing a high-quality graphene layer, by encapsulating a sheet of graphene between two pieces of hexagonal boron nitride (hBN) crystals, enables one to investigate the intrinsic carrier transport in the material. Here, I present our recent studies on gate-defined valley-symmetric one-dimensional (1D) carrier guiding in ballistic monolayer graphene [1] and valley-symmetry-protected topological 1D transport in ballistic bilayer graphene [2]. For the first topic, successful carrier guiding was realized by inducing a high distinction (~ more than two orders of magnitude) in the carrier density between the region of a quasi-1D channel and rest of the regions in ballistic monolayer graphene. Conductance of a channel shows quantized values in units of $4e^2/h$, where the factor 4 comes from the valley and spin degeneracy. For the second topic, the topological 1D conduction was realized between two closely arranged insulating regions with inverted band gaps, induced under a pair of split dual gating with polarities opposite to each other. The maximum conductance showed $4e^2/h$, again the factor 4 arising from the valley and spin degeneracy. Results of these studies pave a useful pathway for the valley-symmetry-preserved carrier guiding in graphene, which is essential for valleytronics applications of graphene but has always been hindered by the absence of gap and the intervalley scattering at the edges in a constricted geometry of the material.

References:

[1] M. Kim, J.-H. Choi, S.-H. Lee, K. Watanabe, T. Taniguchi, S.-H. Jhi, and H.-J. Lee, Nature Physics DOI:10.1038/Nphys 3804 (2016).

[2] J. Lee, K. Watanabe, T. Taniguchi, and H.-J. Lee, accepted in Scientific Reports.

INVITED TALK #5

Basic of Nuclear magnetic resonance and its application to solid state physics

Atsushi Kawamoto, Yohei Saito, Takuya Kobayashi

Hokkaido University,

Nuclear Magnetic Resonance (NMR) is a powerful tool for science, Medical and Engineering. In solid state physics field, NMR works as a microscopic magnetic detector with atomic scale and provides useful information not only for static characters but also for dynamics on electron spins.

First, I would like to mention about basics of NMR and how it works as magnetic probe in samples. Then I will introduce the application to the magnetism of organic conductors which are research projects in our laboratory.

As an actual example, I will talk about

"^{13}C NMR study of antiferromagnetic fluctuation in organic superconductor λ-$(D)_2GaCl_4$ system".

The λ-type organic conductors, λ-$(BETS)_2MX_4$, [BETS:bis(ethylenedithio) tetraselena fulvalene] consist of donor molecules with the tetrahedral anions MX_4 (M=Ga, Fe ; X=Cl, Br) to become charge-transfer salts of 2D layered structures. With the charge transfer of one electron per two donor molecules, these compounds provide quasi-2D electronic systems and two BETS molecules form a dimer in the conducting layer. The λ-$(BETS)_2GaCl_4$ shows superconductivity below 8 K at ambient pressure. The *d*-wave SC gap structure was reported by a specific heat measurement. The superconducting state persists under higher magnetic field applied just parallel to the conducting layers and the possible Fulde-Ferrell-LarkinOvchinnikov (FFLO) state appears near critical filed Hc_2. The λ-$(BETS)_2FeCl_4$, which is isostructural with λ-$(BETS)_2GaCl_4$ is an insulator in the zero magnetic field. However, when a strong magnetic filed is applied parallel to the conducting layers, a superconductivity appears, which is called field induced (FISC) state. The possible FFLO also appears at the phase boundary of FISC phase. In normal state of λ-$(BETS)_2GaCl_4$, antiferromagnetic (AF) spin fluctuation and charge disproportionation were discussed by ^{1}H and ^{77}Se NMR, however, the paring mechanism of λ salts is still unclear due to lack of the universal phase diagram. In strongly correlated electron systems, the nature of the insulating phase in the vicinity of the SC phase is closely related with the superconductivity. Mori *et al.* investigated the ground state of λ-D_2GaCl_4 systems using the molecular substitution and suggested a universal phase diagram of λ-type salts. The substitution with *D*= us-BEDT-STF [us-BEDT-STF: unsymmetric-bis(ethylenedithio) diselenadithiafulvalene] and *D*= BEDT-TTF [BEDT-TTF: bis(ethylenedithio)tetrathiafulvalene] can control the band-width changing the transfer integral between molecules. They revealed that the ground state of λ-(us-BEDT-STF)$_2GaCl_4$ situating near λ-$(BETS)_2GaCl_4$ is insulating and the possibility of the anti-ferromagnetic ground state of BEDT-TTF salts. Recently, Minamidate *et al.* realized the superconductivity of λ-(us-BEDT-STF)$_2GaCl_4$ under the pressure verifying the bandwidth control [1]. The ground state of λ-(us-BEDT-STF)$_2GaCl_4$ under an ambient pressure is of significant research interest for discussing the nature of the superconductivity and confirming the anti-ferromagnetic ground state of λ-$(BEDT)_2GaCl_4$. Until now, magnetic susceptibility measurement of λ-(usBEDT-STF)2GaCl4 was performed and found that λ-(us-BEDT-STF)$_2GaCl_4$ shows no magnetic ordering down to 2 K. Since NMR is one of these purposes, we investigate the ground state of λ-(us-BEDT-STF)$_2GaCl_4$ and λ-(BEDT-TTF)$_2GaCl_4$ including λ-(BETS)$_2GaCl_4$ using the site-selective ^{13}C NMR.

TALK #18

Ab-initio studies of polymorphism and phase transition in MoS_2

Sera Jeon[1], Jaekwang Lee[1*]

[1]Department of Physics, Pusan National University, Busan, Republic of Korea

Recently, MoS_2 has been widely studied due to its relatively simple fabrication and much functionality with other materials in many areas. In particular, one of the most interesting properties of MoS_2 is polymorphism that MoS_2 can exist in various phases with distinct properties such as semiconducting 2H-MoS_2, metallic 1T-MoS_2. 1T'-MoS_2, 1T''-MoS_2. Here, using first principles calculations, we investigate the electronic properties and lattice dynamics of each phases, and systematically estimate the required energy for phase transition between 2H and 1T, 1T', 1T''. We expect that our studies can provide the fundamental information to understand polymorphism and phase transition in various transition metal dichalcogenides(TMDs).

*** Corresponding author: jaekwangl@pusan.ac.kr**

TALK #19

Magnetic properties of $S = 5/2$ triangular lattice dimer $Cs_3Fe_2Cl_9$

[1]Y. Ishii, [2]Y. Matsushita, [1]H. Yoshida, [1]M. Oda, [3]M. Hagihala, [4]T. Masuda, [5]T. Kida, [5]Y. Narumi, and [5]M. Hagiwara.

[1]*Dept.of Phys.Grad.Sch.Sci., Hokkaido Univ.*, [2]*National Institute for Material Science*, [3]*KEK − IMSS*, [4]*ISSP*, [5]*AHMF.Dept.of Phys.Grad.Sch.Sci.Osaka Univ.*

$Cs_3Fe_2Cl_9$ is one of the members of $A_3M_2X_9$ (A = Cs, Rb ; M = Ti, V, Cr, Fe ; X = Cl, Br, I) series compounds. The crystal structure consists of the triangular lattice made of $(Fe_2Cl_9)^{3-}$ dimers (Fig. 1 (a)). Three dominant magnetic interactions, the intra-dimer interaction J_0, and the inter-dimer interactions J_p, J_c are considered in this system[1]. These competing interactions can evoke exotic phenomena.

We succeeded in synthesizing the single crystals of $Cs_3Fe_2Cl_9$ by the hydrothermal synthesis and measured the magnetic properties and the heat capacity on the single crystal. In the previous reports, the magnetic susceptibility of the powder sample showed no magnetic order[2]. However, our magnetic and heat capacity measurements on the single crystal revealed that $Cs_3Fe_2Cl_9$ exhibited the antiferromagnetic long-range order at $T_N = 5.3$ K under zero magnetic field. Unlike a normal antiferromagnetic transition, the easy-axis (c-axis) magnetic susceptibility showed the sudden drop at T_N and then it decreased toward zero with T-linear temperature dependence (Fig. 1 (b)). Increasing magnetic field, the susceptibilities below T_N show drastic changes (Fig. 1 (b)). In addition, the magnetization show the metamagnetic transitions and the 1/2 magnetization plateau (Fig. 1 (c)).

In my presentation, I will show more detail experimental results and discuss the magnetism of $Cs_3Fe_2Cl_9$.

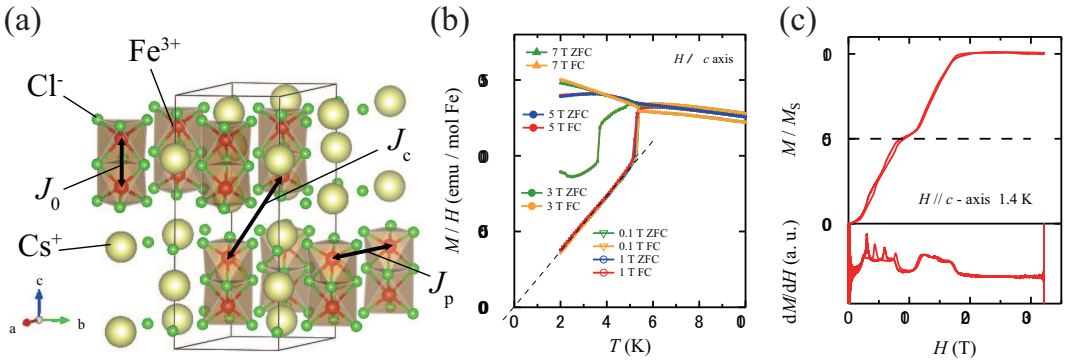

Fig. 1: (a)The perspective view of the crystal structure of $Cs_3Fe_2Cl_9$. (b)The magnetic susceptibilities of $Cs_3Fe_2Cl_9$ under several fields (H // c - axis). (c)The high field magnetization (upper side) and the field differential of the high field magnetization (lower side) at 1.4 K (H // c - axis).

References

[1] B Leuenberger and Hans U. Güdel, Journal of Solid State Chemistry, 64, 90-101 (1986).

[2] A. P. Ginsberg and M. B. Robin, Inorg. Chem., 2, 817-822 (1963).

TALK #20

Muon Spin Resonance Investigation on the Magnetic Order of π-electrons in the Rubidium Superoxide (RbO_2)

Fahmi Astuti[1,2], Dita P. Sari[1,3], Retno Asih[1,3], Mizuki Miyajima[4], Takeshi Kakuto[4], Takehito Nakano[3], Yasuo Nozue[3], Isao Watanabe[1,2,3], and Takashi Kambe[4]

RIKEN Nishina Center[1], Hokkaido University[2], Osaka University[3], Okayama University[4]

Rubidium superoxide is one of alkali metal superoxides (AO_2; A = Na, K, Rb, and Cs). The magnetic properties of these systems result from the partially filled p-electron levels of the superoxide anion O_2^-. In the O_2^-, three electrons occupy a pair of degenerate antibonting π* molecular orbitals; thus, there is one unpaired spin ($S = 1/2$). All AO_2 compounds undergo structural distortions splitting the degeneracy of the π* on cooling [1]. In the case of CsO_2, a magnetic ordering is observed below 10 K [2,3]. We have confirmed this ordered state to be a long-range one by using μSR. The magnetic order was observed at the temperature below ~ 9 K. This system also provides rare simple manifestations of the coupling between spin, lattice, and orbital degrees of fredom [4].

We also studied another alkali metal superoxide, RbO_2. We have checked the sample quality by the X-ray powder diffraction and the magnetic properties by susceptibility measurements. We have carried out the ZF- and LF-μSR measurements to investigate the magnetic order in RbO_2. As the temperature decreases, the time spectrum started to change and the muon-spin precession behavior appear below about 15 K. In our presentation, we are going to report detailed results recently achieved in RbO_2, in conjunction with the results in CsO_2.

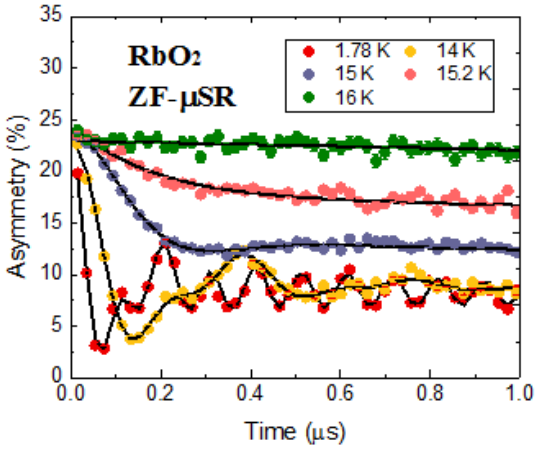

Figure 1. Zero-field time spectrum of RbO_2 at the various temperature.

References:
[1] S. Riyadi et al., Phys. Rev. Lett. **108**, 217206 (2012).
[2] A. Zumsteg et al., Phys. Cond. Matter **17**, 267 (1974).
[3] M. Klanjsek et al., PRL **115**, 057205 (2015).
[4] T. Knaflič et al., PRB **91**, 174419 (2015).

TALK #21

Model search in superstring theory

Takuya Tatsuishi

Department of Physics, Hokkaido University

In particle physics, the Standard Model (SM) is well established and which is the most fundamental theory to explain elementary particles and three forces (except for gravity) in nature. However, many mysteries remain in this field. Superstring theory is one of the candidates for solving these mysteries. Since the SM is precisely confirmed by experiments, superstring theory must contain the SM. Superstring theory has many theoretical parameters as their background space-time structure. We are searching for appropriate space-time structures in superstring theory to lead the SM. In this talk, I will show you whole picture of our study.

TALK #22

ESR Study of the Valence Bond Solid material $EtMe_3P[Pd(dmit)_2]_2$

Sunghyun Kim[1,2] , **Yugo Oshima**[1,2] , **Reizo Kato**[2]

Hokkaido Univ.[1], *RIKEN*[2]

When the spins are located at each corner of a triangle and are antiferromagnetically aligned (i.e. antiparallel), the first two spins can be aligned antiparallel, however, the third spin becomes frustrated since it can not be aligned antiferromagnetically. This is known as the geometrical frustration. Therefore, the magnetic ground state of S=1/2 antiferromagnetic triangular lattice has been debated for the past few decades in condensed matter physics. The anion radical salt $X[Pd(dmit)_2]_2$ (X is a monovalent cation) is one of the material which has S=1/2 antiferromagnetic triangular lattice. Wide variety of ground states, such as quantum spin-liquid state, antiferromagnetic state, charge-ordered state have been observed depending on the degree of geometrical frustration controlled by the monovalent cation X [1]. Recently, a novel salt $EtMe_3P[Pd(dmit)_2]_2$ has been synthesized. It is known from the magnetic susceptibility measurement that $EtMe_3P[Pd(dmit)_2]_2$ turns into a valence bond solid (VBS) state at T_{VBS}=25 K which is similar to the spin-Peierls state. The spin gap between the singlet and triplet states obtained by the magnetic susceptibility measurement is 40 K [2]. However, the spin gap of 40 K seems to be small comparing to the transition temperature T_{VBS}=25 K. ESR is one of the sensitive probe that can deduce the spin gap from the temperature dependence of integrated intensity. Therefore, we have performed ESR measurements of $EtMe_3P[Pd(dmit)_2]_2$ to determine the spin gap of the VBS state. Moreover, the ESR signal below 25 K shows unconventional lineshape (Fig.1). Although the spin density is very low, this anomaly of the lineshape can only be explained from two Lorentzian ESR signals which have different linewidth (Fig.2). This suggests that two different kind of spins exist below 25 K. Detailed analysis of our ESR results will be presented, and its magnetic properties will be discussed.

Reference

[1] R. Kato, Bull. Chem. Soc. Jpn., 87 (2014) 355-374.
[2] M. Tamura, A. Nakao and R. Kato, J. Phys. Soc. Jpn., 75 (2006) 093701

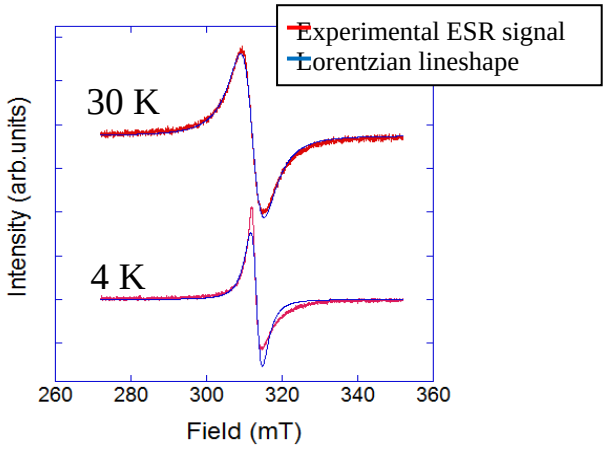

Figure 1. ESR signals at 4 K and 30 K (g_{max})

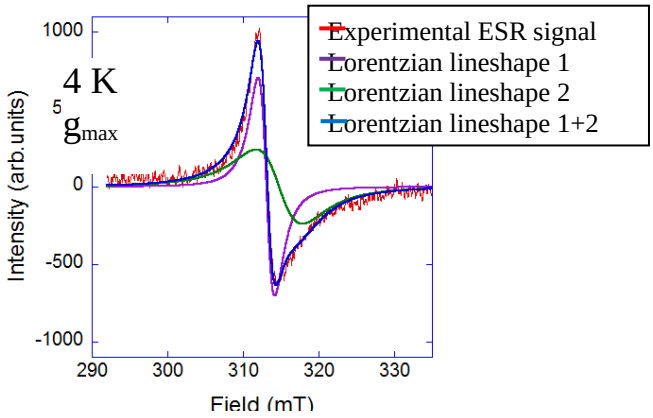

Figure 2. Two Lorentzian ESR signals

INVITED TALK #6

Advantage and Limit of First-principles Electronic Structure Calculation for Material Science

Chul-Hong Park

Department of Physics Education/&Research Center for Dielectric and Advanced Matter Physics, Pusan National University, Busan 609-735, Korea

cpark@pusan.ac.kr

The first-principle electronic calculations are now widely applied for the investigation of the microscopic properties of materials such as semiconductor, magnetic material, and recently two-dimensional materials, since the various software for the material calculation are easily accessible and the computations are also easy, and the computer technology is well developed. The brief history and the basic knowledge of the first-principles calculation will be introduced, and the power and the advantage, and the limit will be discussed.

TALK #23

μSR Studies on Electron Dynamics in Guanine

Harison Rozak[1,2], Fadhilah Zaharim[2], Fahmi Astuti[1,3], Retno Asih[4], Eliana Ismail[2], Amira Abu Bakar[2], Shukri Sulaiman[2], Mohamed Ismail Mohamed-Ibrahim[2] and Isao Watanabe[1,3,4]

RIKEN Nishina Center[1], Universiti Sains Malaysia[2], Hokkaido University[3], Osaka University[4],

The muon-spin relaxation (μSR) technique can be used to study of the electron transport phenomena in DNA at the microscopic level [1-3]. We are applying this method in order to investigate relationships between damages on DNA and the ageing process. It can be suggested that damages on the DNA which causes ageing would affect the electron transfer along the DNA chains. At this moment, the electron transfer along the DNA chains has not yet been well studied by using microscopic tools. We expect that changes in the electron transfer along the DNA chains can be observed in the relaxation behavior of the muon-spin polarization as observed in past studies [1-3]. Since real DNA molecules are huge and too complicated, it is almost impossible to sense the electron transfer along DNA chains by only small numbers of muons. Thus, for our study, we choose single strands of synthetic DNA (consisting of only 12 mer guanine bases) in order to see the basic behavior of the electron transfer along only one type of nitrogen base.

μSR experiments were carried out at the RIKEN-RAL Muon Facility in the UK covering the temperature range from 300 K down to 100 K with longitudinal fields (LF) up to 4,000 G. LF was applied along the initial muon-spin polarization. It has been observed that the muon-spin-relaxation rate is proportional to the minus square-root against LF. This behavior can be characterized as the result of the 1-dimensional diffusion of electrons along single strand DNA [3]. We also carried out μSR in the transverse field (TF) of 3G. The figure below shows the time spectrum at 300 K in TF=3 G. There seems to be the muon-spin precession with enhanced internal field. This result shows a possibility of the formation of the so-called muonium state. This enhanced hyperfine field at the muon site can be used to investigate the muon position on the DNA molecule.

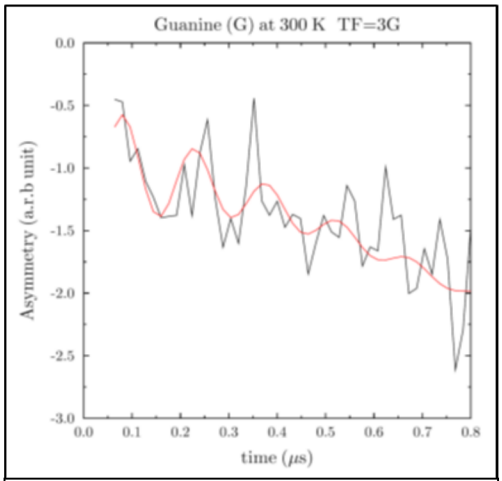

Figure: Time spectrum measured in Guanine (G) under TF=3 G at 300 K.

References **:**

1) K. Ishida et.al, Phys. Rev. Lett. 55, 2009 (1985).

2) K. Nagamine et.al, Phys. Rev. Lett. 53, 1763 (1984).

3) E. Torikai et al., Hyperfine Interact. 138, 509 (2001).

TALK #24

Hysteretic response to electric current observed in toroidal magnetic ordered state on UNi_4B

[A]*Grad. School of Science, Hokkaido Univ.,* [B]*KEK IMSS CMRC,* [C]*UK MFF*

H. Saito[A], N. Miura[A], H Hidaka[A], T. Yanagisawa[A], H. Amitsuka[A], C. Tabata[B], M. Vališka[C], K. Uhlířová[C], J. Prokleška[C], and V. Sechovský[C]

Toroidal moment ***t*** is one of the parameters that describes the strength of the magnetoelectric coupling. It is defined as the vector product of position ***r*** and spin ***S***. It can be found in the Taylor expansion of Helmholtz free energy with respect to electric field and magnetic field. In other words, toroidal moment ***t*** is one of the basic notions in electromagnetism. In the last decade, the toroidal order, which is the ordered periodic array of toroidal moments, has attracted much interest in connection with multiferroic insulating materials. Recently, S. Hayami *et al*. showed theoretically that such an exotic order can occur also in metallic systems, and exotic phenomena such as magnetization induced by electric current can occur in the toroidal ordered metal [1].

UNi_4B is one of the candidate metals for the toroidal order. The orthorhombic structure in the present compound (symmetry: *Cmcm*, D_{2h}^{17}, No. 63) is the structure slightly distorted from hexagonal coordinates[2]. Since it is difficult to detect the distortion by Laue photography on single crystal, we assume the structure as hexagonal in the present work. Below T_N (= 20.4 K), it is suggested that it orders antiferromagnetically in a magnetic structure where the magnetic moments carried by the 2/3 of U ions make the vortices in each triangular planes [3]. This magnetic structure is the same as that assumed in the above theory. In order to test the theory, we have performed magnetization measurements under electric current on UNi_4B. We observed that magnetization is induced by constant electric current in the ordered state of UNi_4B [4]. Therefore, the validity of the theory is confirmed in part by the experiments.

However, the accuracy of the previous measurements is not high because of the existence of the magnetic field generated by applied electric current during the measurement. In order to achieve higher accuracy, we have tried magnetization measurement after applying square-wave pulsed current ("pulsed-current magnetization measurement") and reported briefly that pulsed-current also cause the change of magnetization below T_N.

Recently, we succeeded in growing higher-quality single crystalline sample of UNi_4B and got the chance to continue above measurements in Charles University, Prague, Czech Republic. The results of pulsed-current magnetization measurement for each settings of $B \parallel a$, b-axes and $J \parallel a$, b, and c-axes will be presented. Then, we'll discuss about the possible cause of the strange response of magnetization to electric current.

This work was supported by JSPS KAKENHI Grant Number JP15H05885 and JP15K21732 (J-Physics). Experiments were performed in the Materials Growth and Measurement Laboratory MGML (see: http://mgml.eu).

[1] S. Hayami, H. Kusunose, and Y. Motome, Phys. Rev. B **90**, 024432 (2014).
[2] Y. Haga, A. Oyamada, T. D. Matsuda, S. Ikeda, and Y. Ōunki, Physica B **403** 900-902 (2008).
[3] S. A. M. Mentink, A. Drost, G. J. Nieuwenhuys, E. Frikkee, A. A. Menovsky, and J. A. Mydosh, Phys. Rev. Lett. **73**, 1031 (1994).
[4] H. Saito, K. Uenishi, N. Miura, C. Tabata, H. Hidaka, T. Yanagisawa, and H. Amitsuka, 20th International Conference on Magnetism (Barcelona), TU.A-P67 (2015).

TALK #25

Deposition temperature-dependent the physical property variations of epitaxial VO_2 film

Dooyong Lee[1,3], Hyegyeong Kim[1], Ji Woong Kim[1], Donghyuk Yang[1], Yunhee Cho[1], Sehwan Song[1], Jong-Seong Bae[2], Kyoung Soon Choi[3], Jouhahn Lee[3], Jaekwang Lee[1] and Sungkyun Park[1,1]

[1]Department of Physics, Pusan National University, Busan 46241, Korea

[2]Busan Center, Korea Basic Science Institute, Busan 46742, Korea

[3]Advanced Nano Surface Research Group, Korea Basic Science Institute, Daejeon 34133, Korea

Abstract

VO_2 films grown on Al_2O_3(0001) substrate were deposited at various temperatures (500 °C ~ 720 °C). As a result, metal-insulator-transition temperature increased with increasing deposition temperature up to 650 °C and sharply decreased with further increasing temperature. X-ray diffraction measurements showed that all films had (020)-oriented phase pure structure. Furthermore, the degree of out-of-plane tensile strain decreased and the crystallinity of films was improved with increasing deposition temperature due to additional thermal energy. X-ray photoelectron spectra revealed that V^{5+} state change to V^{4+} state from 500 °C to 650 °C and V^{4+} state change to V^{3+} state above 650 °C. From the detailed optical band gape examination using UV-Vis and Ultraviolet photoelectron spectroscopy, the optical band gap of VO_2 films could be divided into three distinct regions depending on the deposition temperature. First, the optical band gap of the films deposited at 500 °C and 550 °C showed between 0.238 and 0.287 eV due to the out-of-plane tensile strain and V^{5+} state. Second, a large band gap region (0.456 eV ~ 0.469 eV) appeared due to the improved crystallinity and V^{4+} state for the films deposited at 600 °C, 650 °C and 700 °C. Lastly, a narrow band gap (~0.209 eV) for the film deposited at 720 °C due to additional electrons created by V^{3+} state. These results provide the insight of MIT characteristics of the epitaxial VO_2 films deposited at various temperatures. This study was supported in part by NRF Korea (NRF-2015R1D1A1A01058672) and Korea Basic Science Institute Research Grant (E37800).

1

Correspondence should be addressed to Sungkyun Park (psk@pusan.ac.kr)

TALK #26

Reconsideration of Muon Sites in La_2CuO_4

M. R. Ramadhan[1,2], R. Asih[1,3], M. I. Mohamed-Ibrahim[4], S. Sulaiman[4], and I. Watanabe[1,2,3,4]

RIKEN Nishina Center[1], Universitas Indonesia[2], Osaka University[3], Universiti Sains Malaysia

Muon spin relaxation (μSR) is a powerful tool to investigate the electronic state of the Cu-based high-T_C superconducting oxides. It is important to understand the μSR data of the base material, La_2CuO_4 (LCO), especially in the magnetically ordered states as it provides an insight for another phases of this material. Although μSR technique can provide information on the local magnetic fields at the muon site, it is not so easy to know about the details of the electronic structure surrounding the muons which are the origin of the local fields at the muon site. This is because we need to know the exact position of muon inside material. Several attempts have been made to tackle this problem in the past [1-3]. However a unified method to know about muon positions in materials has not yet been established.

We are trying to find a way to estimate muon positions by using μSR experimental data in conjunction with the density functional theory (DFT) calculations. We are now carrying out detailed DFT calculations on LCO using the electronic correlation function with the on-site Coulomb repulsive interaction, GGA + U. We also take into account a quantum phenomena of the muon itself as a fine particle (zero-point vibration motion of muon) which depends on the shape of the surrounding electrostatic potential. We also include the effect of the local deformation of the crystal structure caused by the presence of muon.

We are carrying out DFT calculations by using the RIKEN cluster supercomputing system named HOKUSAI [4]. In our presentation, we will discuss our recent computational results and discuss the progress of our calculation processes and achievements.

References:
[1] R. Saito, et al.: Physica C **185-189** :1217-1218 (1991).
[2] S. Sulaiman, et al. : Phys. Rev. B **49** : 9879 - 9884 (1994).
[3] Suter, et al.: Physica B **326** : 329-332 (2003).
[4] HOKUSAI Greatwave : http://www.riken.jp/pr/press/2015/20150403_1/

TALK #27

Analysis for high-T_c superconductors based on self-consistent perturbation expansion

Department of Physics, Hokkaido University
Hiroki Morita, Takafumi Kita

The mean-field Bardeen-Coopper-Schriffer (BCS) theory has been successful describing superconductivity in metallic superconductors quantitatively. But now, we have many superconductors where interactions are stronger beyond the applicability of the mean-field theory such as cuprate superconductors. So, much effort to go beyond the BCS theory has been made, and one of them is FLEX-S approximation.

FLEX-S approximation is classified as a perturbation theory. In the FLEX-S approximation, we incorporate strong correlation effects by incorporating higher-order terms into the self-energy. Furthermore, the FLEX-S approximation is an extension of fluctuation-exchange (FLEX) approximation which has been successful in describing anomalous normal-state transport phenomena of high-T_c superconductors. Note in this context that FLEX-S approximation satisfies various conservation laws naturally.

This time, We calculate the spectral function in both normal and anomalous states for the YBCO model based on the FLEX-S approximation.

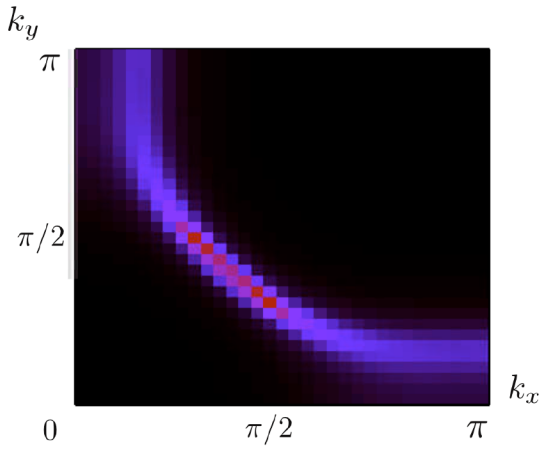

Fig.1 The Fermi surface of the YBCO model. We can see Fermi arc near $k_x \sim k_y$

[1] T. Kita; JPSJ **80**, 124704 (2011).

TALK #28

Investigation of the electron band structure of single-crystal SnSe

Ji–Eun Lee[1], Jinwoong Hwang[1], Hyejin Ryu[2], Dung Anh Tuan[3], Sunglae Cho[3], Sung-Kwan Mo[2], and Choongyu Hwang[1*]

**Corresponding author: ckhwang@pusan.ac.kr*

[1]*Department of Physics, Pusan National University, Busan 46241, South Korea*

[2]*Advanced Light Source, Lawrence Berkeley National Laboratory, Berkeley, CA 94210, USA*

[3]*Department of Physics, University of Ulsan, Ulsan 680-749, South Korea*

SnSe is a new promising thermoelectric material which can directly convert discarded heat into electricity. The performance of thermoelectric materials is defined as the dimensionless figure of merit $ZT = (S^2 \sigma/\kappa)T$ where S, σ, κ and T are the Seebeck coefficient, electrical conductivity, thermal conductivity, and temperature, respectively. There have been a lot of efforts to enhance the ZT value, e.g., increase the power factor ($S^2 \sigma$) or decrease κ. However, it is challenging to achieve high power factor and low thermal conductivity, simultaneously. Recently, it has been experimentally discovered that single-crystal SnSe shows low thermal conductivity and unique charge transport properties, resulting in the highest thermoelectric performance. Extremely low thermal conductivity originates from anharmonic bondings. Unique charge transport properties are attributed to multi-valley valence bands, which has been proposed theoretically but not proven experimentally. Here we report an angle-resolved photoemission study on single-crystal SnSe. The electron band of SnSe is highly anisotropic with multiple valleys near the valence band maximum, mostly consistent with previous theoretical works.